

## Electronic Supplementary Information (ESI)

### **General Construction of Asymmetric Bowl-Like Hollow Nanostructures by Grafting Carbon-Sheathed Ultrasmall Iron-Based Compounds On Carbon Surface as Superior Anode for Sodium-Ion Hybrid Capacitors**

*Jingyu Gao,<sup>a</sup> Yapeng Li,<sup>a</sup> Bo Peng,<sup>a</sup> Gongrui Wang<sup>a</sup> and Genqiang Zhang\*<sup>a</sup>*

<sup>a</sup> *Hefei National Laboratory for Physical Sciences at the Microscale, CAS Key Laboratory of Materials for Energy Conversion,*

*Department of Materials Science and Engineering, University of Science and Technology of China, Hefei, Anhui 230026 China.*

*\*Correspondence: gqzhangmse@ustc.edu.cn*

## 1. Experimental section

### 1.1 Synthesis

*Synthesis of bowl-like RF templates:* The bowl-like RF particles are synthesized through a modified procedure according to previous literature.<sup>1</sup> In a typical synthesis, tetraethyl orthosilicate (TEOS, 2.8 mL), resorcinol (0.4 g), and formalin (37 wt %, 0.56 mL) were dissolved into the mixed solution composed of ethanol (70 mL), deionized water (10 mL) and ammonia aqueous solution (3.0 mL, 28 wt %) followed by stirring for 6h. Then, another addition of 1.5 mL of TEOS is performed followed by another 24 h stirring. After this, the mixture was transferred to 100 mL Teflon-lined autoclave and treated at 100 °C for 24 h in the electric oven. Then, the SiO<sub>2</sub>@RF spheres were collected after washing with DI water and ethanol several times. Finally, the bowl-like RF particles can be spontaneously formed after the removal of SiO<sub>2</sub> with 2M NaOH solution or 4h at 70 °C.

*Synthesis of bowl-like C@FeX(X=O/S/Se/P):* The synthesis of bowl-like C@FeX hollow particles are achieved through a two-step strategy. First, 30 mg of bowl-like RF template were well dispersed into a solution of 30 mL ethylene glycol (EG) dissolved with 0.4 mmol of Fe(CH<sub>3</sub>COO)<sub>2</sub>·4H<sub>2</sub>O by sonication. The mixed solution was then refluxed at 170 °C for 2 h in an oil bath to form the conformally coated Fe-glycolate layer on the surface of RF template (RF@Fe-glycolate). The intermediate products were then collected by centrifugation followed by washing with deionized water and ethanol for several times. The final product of bowl-like C@FeX hollow particles can be obtained through the conventional vapor-phase conversion process. Specifically, for the synthesis of bowl-like C@FeSe<sub>2</sub> hollow particles, 25 mg of RF@Fe-glycolate and 50 mg of Se powders were separately put into both ends of a quartz boat, further transferred into a tube furnace, followed by thermal annealing treatment at 350 °C for 2h then 500 °C for another 2 h under the protection of Ar. For comparison, pure carbon bowl was obtained by the same annealing treatment. The formation of C@FeS is performed using a dual-temperature zone tube furnace, where S powder located at the upstream side of the furnace is heated to 200 °C while the RF@Fe-glycolate located at downstream is heated to 400 °C. For the synthesis of bowl-like C@FeP hollow particles, 10 mg of C@Fe-glycolate and 200 mg of NaH<sub>2</sub>PO<sub>2</sub> were separately put into two quartz boat, where were then heated up to 300 °C for 2h and then 600 °C for another 2h under Ar protection. The C@Fe<sub>3</sub>O<sub>4</sub> were synthesized by direct thermal annealing treatment of RF@Fe-glycolate at 500 °C for 24h under Ar atmosphere.

### 1.2 Materials Characterization

The crystal structure of samples was tested by X-ray diffraction (XRD, TTR-III, Japan) using Cu–K $\alpha$  radiation. Field-emission scanning electron microscopy (FESEM, JSM-6700F, Japan) and transmission electron microscopy (TEM, H-7650, Japan; Talos F200X, USA) were utilized to analyze the morphology and structure of the synthesized materials. Nitrogen sorption isotherms were characterized by the Surface Area and Porosity Analyzer (ASAP 2020). The valence of several elements was investigated by X-ray photoelectron spectroscopy (XPS, ESCALAB 250, USA).

### 1.3 Electrochemical Measurement

The electrochemical tests were carried out in CR2016 coin-type cells. The electrode was prepared by mixing bowl-like C@FeX hollow particles, carbon black (Super-P) and sodium carboxymethylcellulose (CMC) in a weight ratio of 7:2:1 on the aluminum foil. The loading mass of active materials is around 1.0-1.2 mg cm<sup>-2</sup>. Metal Na foil was used as both reference and counter electrode. Different electrolytes were used for different materials: For C@FeSe<sub>2</sub> electrode, 1 M sodium trifluoromethanesulfonate (NaCF<sub>3</sub>SO<sub>3</sub>) in DEGME was used as the electrolyte. For C@Fe<sub>3</sub>O<sub>4</sub> and C@FeP, 1M NaClO<sub>4</sub> in propylene carbonate (PC) was used as electrolyte. Cyclic voltammetry (CV) measurement was performed on a CHI660E electrochemical workstation. Galvanostatic discharge/charge tests were conducted on a NEWARE battery tester at 0.5-2.9V for C@FeSe<sub>2</sub> and 0.01-3V for C@Fe<sub>3</sub>O<sub>4</sub> and C@FeP.

### 1.3 Fabrication of Sodium-based Hybrid Capacitors

For the sodium-based hybrid capacitors (NIHCs), the activated carbon (AC, 80 wt%), additive carbon black (10 wt%) and polyvinylidene fluoride (PVDF, 10 wt%) binder were mixed in N-methyl-2-pyrrolidone (NMP) solution followed by coating on an Al foil. For the anode, the C@FeP electrodes in Na-half cells was precycled for five times at 0.1 A g<sup>-1</sup>, and then the cells were dismantled in the glove box. The NIHCs were then built by assembling the preactivated C@FeP anode and the AC cathode in CR2016 coin cells with the same separator and electrolyte as that in half cells. The mass ratio of the two electrodes (anode/cathode) was 1:3. The charge and discharge process of the NIHCs device were performed on the voltage range of 0-4 V. The specific energy and power density of the NIHCs were calculated by using the equations as follows:

$$E = \int_{t_1}^{t_2} IV dt = \Delta V \frac{I}{m} t$$

$$P = \frac{E}{t} = \Delta V \frac{I}{m}$$

$$\Delta V = (V_{\max} + V_{\min}) / 2$$

Where E (Wh kg<sup>-1</sup>) is the energy density and P (W kg<sup>-1</sup>) is the power density. I is the constant discharge current (A), t<sub>1</sub> and t<sub>2</sub> are the start and end of discharge time (s), and t is the time period for a full discharge (s). V<sub>max</sub> is the potential at the beginning of discharge after the IR drop, V<sub>min</sub> is the terminal voltage in the discharge process. m is the total mass of the active material in both anode and cathode.

2. Supplementary figures

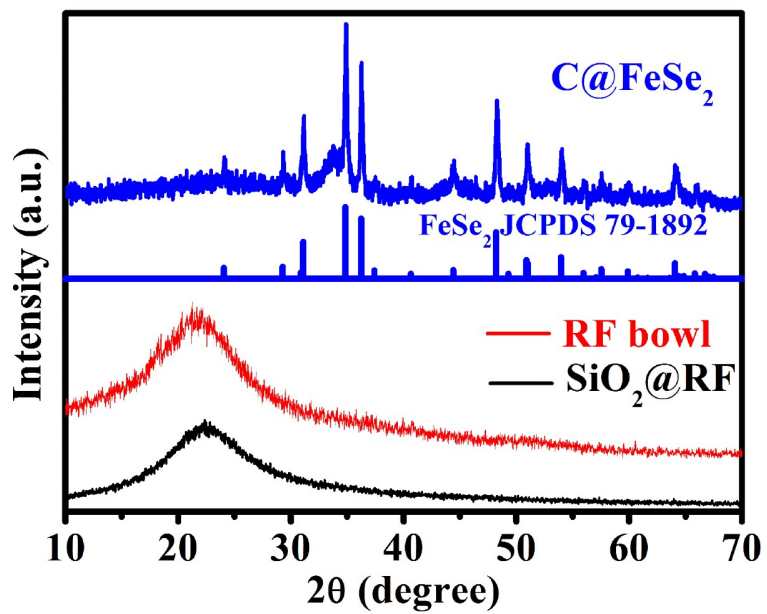
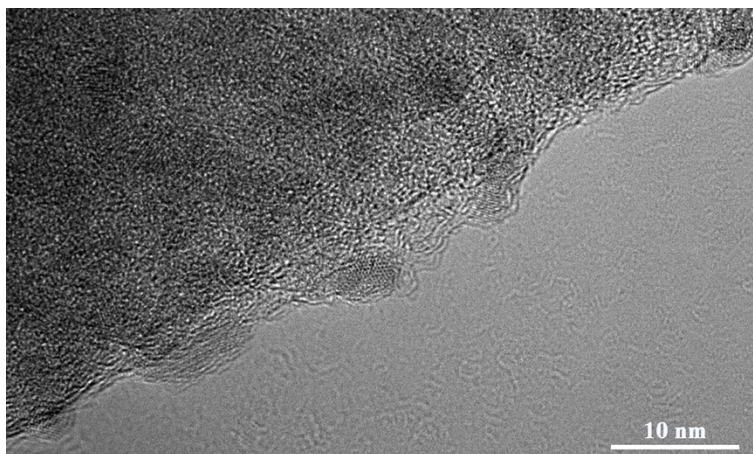


Figure S1. XRD patterns of SiO<sub>2</sub>@RF sphere, bowl-like RF hollow particles and bowl-like C@FeSe<sub>2</sub> particles.



**Figure S2.** HETEM analysis of bowl-like C@FeSe<sub>2</sub> hollow particles taken specifically on the edge of the particle.

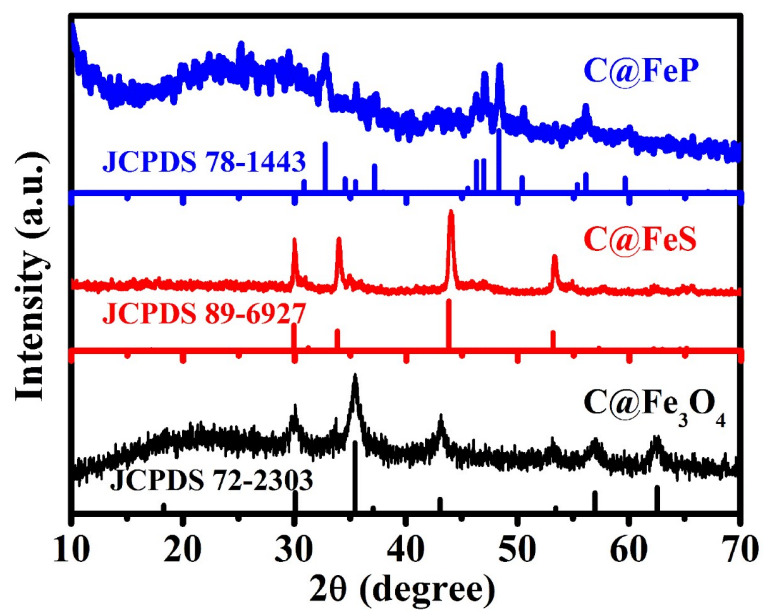
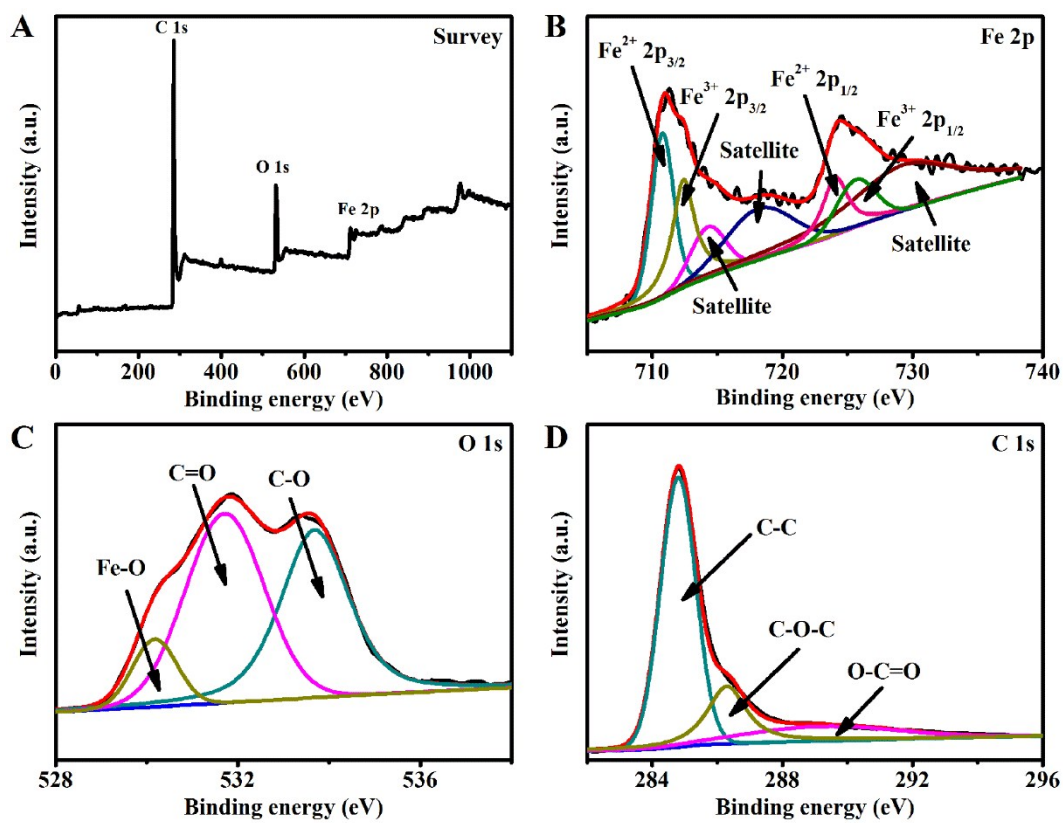
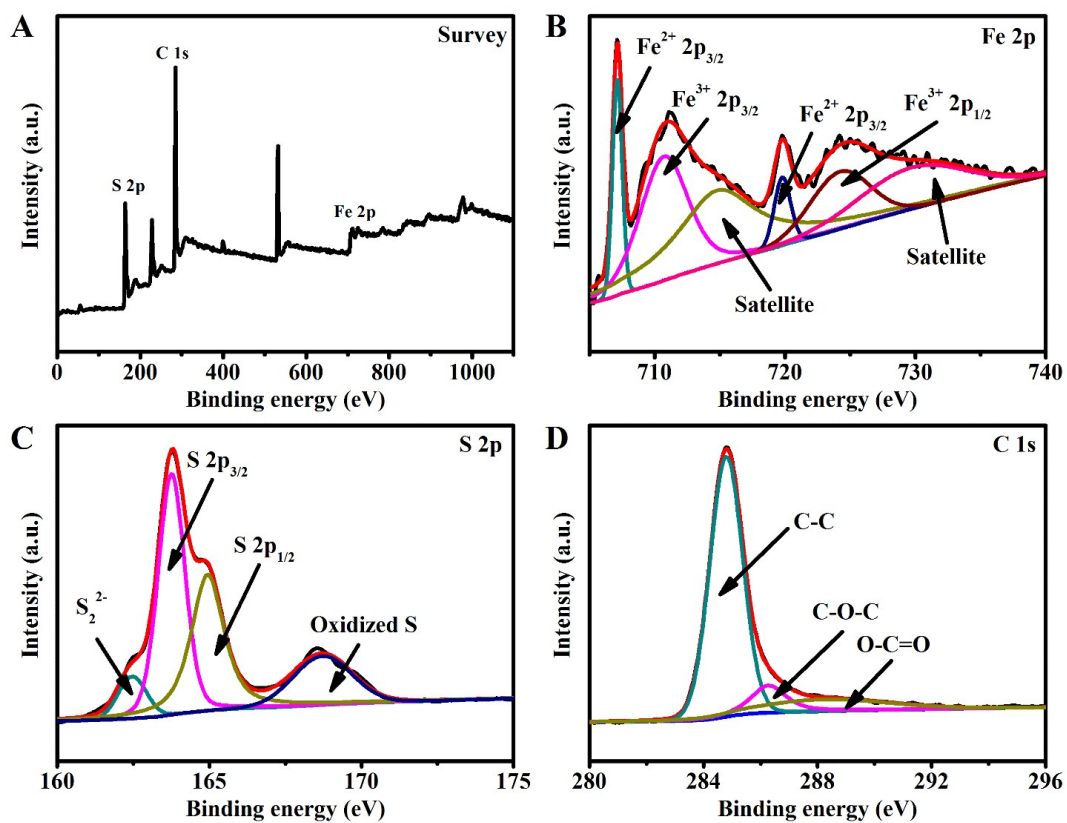


Figure S3. XRD patterns for bowl-like C@Fe<sub>3</sub>O<sub>4</sub>, C@FeS and C@FeP.



**Figure S4.** The XPS analysis for bowl-like C@Fe<sub>3</sub>O<sub>4</sub> hollow particles: A) survey spectrum; B) Fe2p; C) O1s and D) C1s.



**Figure S5.** The XPS analysis for bowl-like C@FeS hollow particles: A) survey spectrum; B) Fe2p; C) S2p and D) C1s.

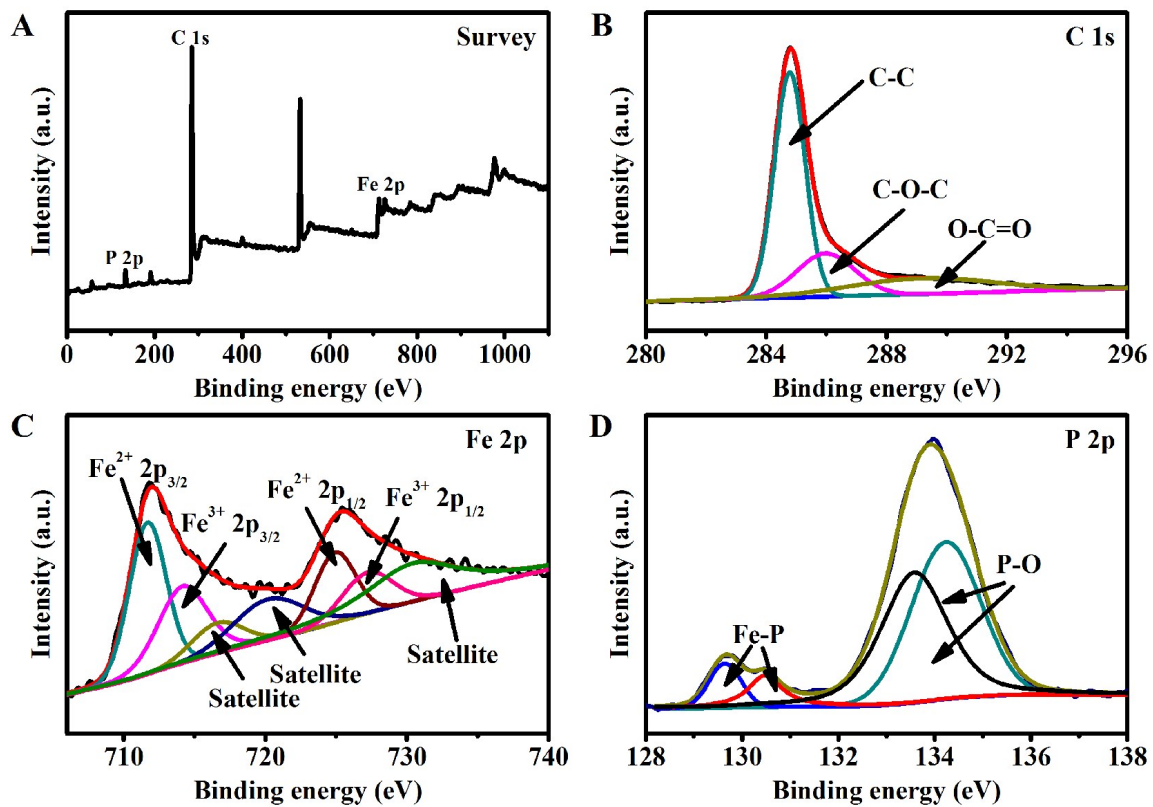


**Figure S6.** The XPS analysis for bowl-like C@FeP hollow particles: A) survey spectrum; B) Fe2p; C) P2p and D) C1s.

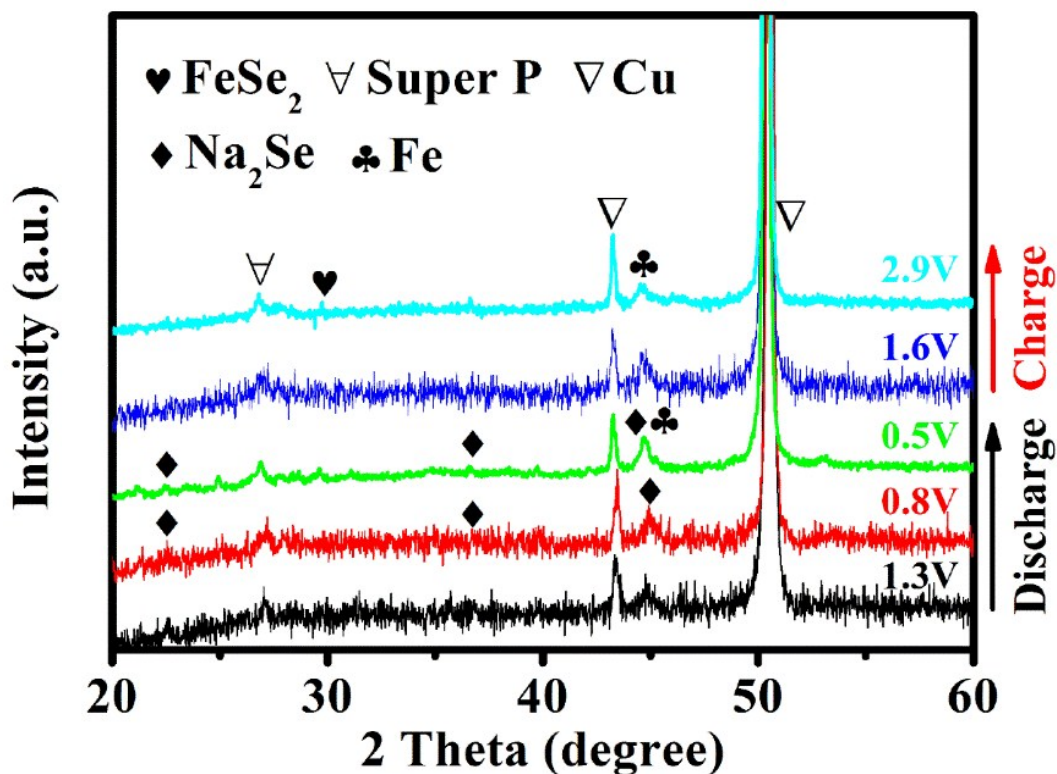


**Figure S7.** Ex-situ XRD analysis of C@FeSe<sub>2</sub> electrode at different charge and discharge states with the corresponding charge–discharge curves.

Notably, there are always two obvious peaks of 43.2° and 50.3° corresponding to the (111) and (200) planes of the Cu current collector. The unique peak of super P is located at 26.6°. During the discharge process from 2.9 to 0.5 V, the new peaks at 22.8°, 37.5° and 44.1° match well with the (111), (220) and (311) planes of Na<sub>2</sub>Se, where the peak of metallic Fe is located at 44.7° reduced from FeSe<sub>2</sub>. In addition, we could barely observe a parallel peak of FeSe under charged to 0.8 V, coinciding with the inconspicuous plateau in discharge process. When charged to 2.9 V, the revived peak of FeSe<sub>2</sub> at 29.3° is indexed to the (011) plane. Moreover, no conspicuous peaks could be observed after discharge to 1.3 V or charge to 1.6 V, which are in accordance with the Na<sub>x</sub>FeSe<sub>2</sub> signal with low crystallinity.

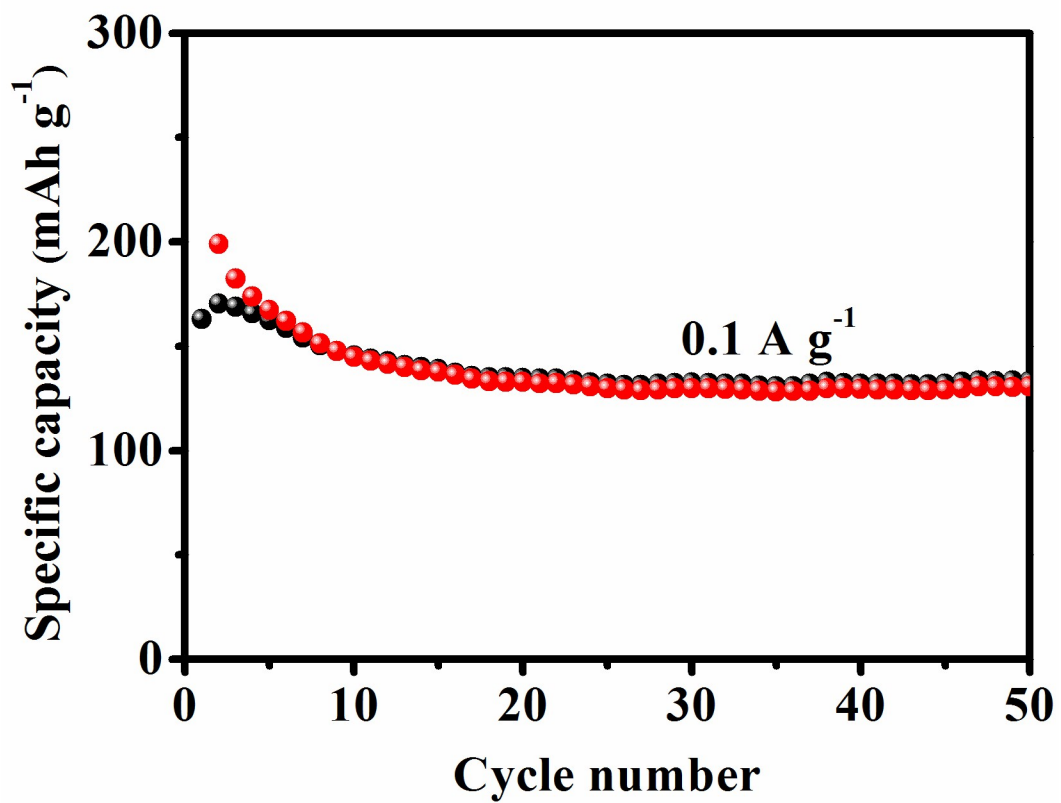


Figure S8. Cycling performance of pure carbon bowl at the current density of 0.1 A g<sup>-1</sup>.

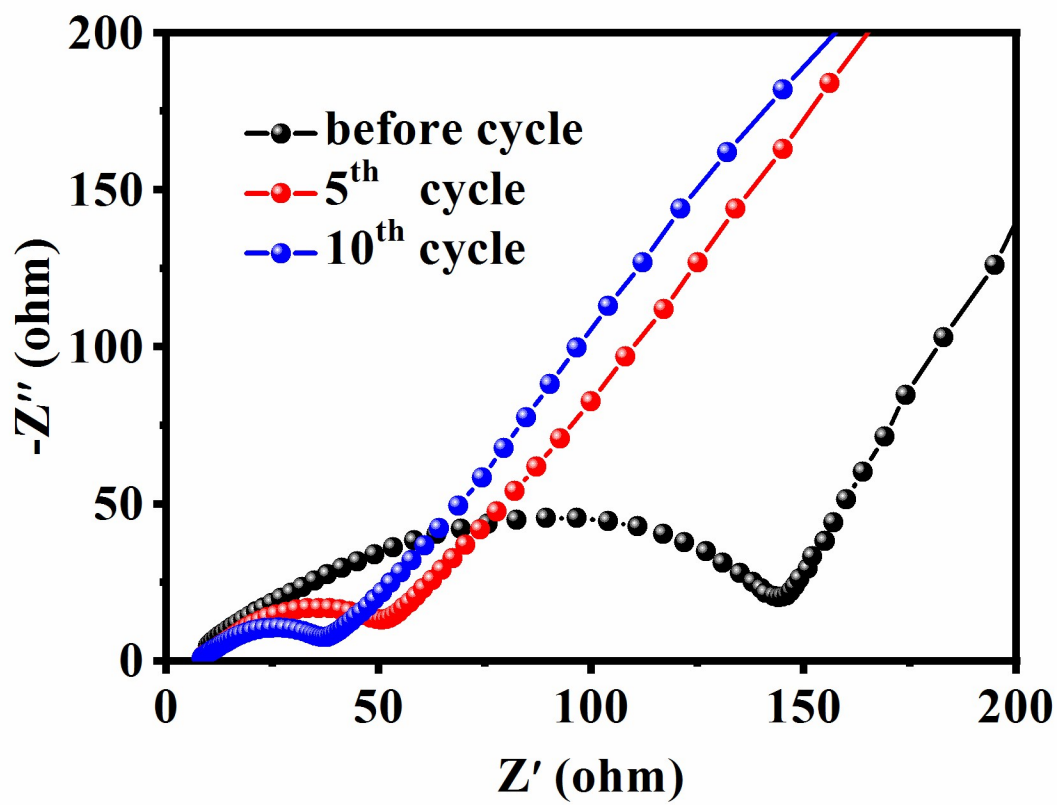
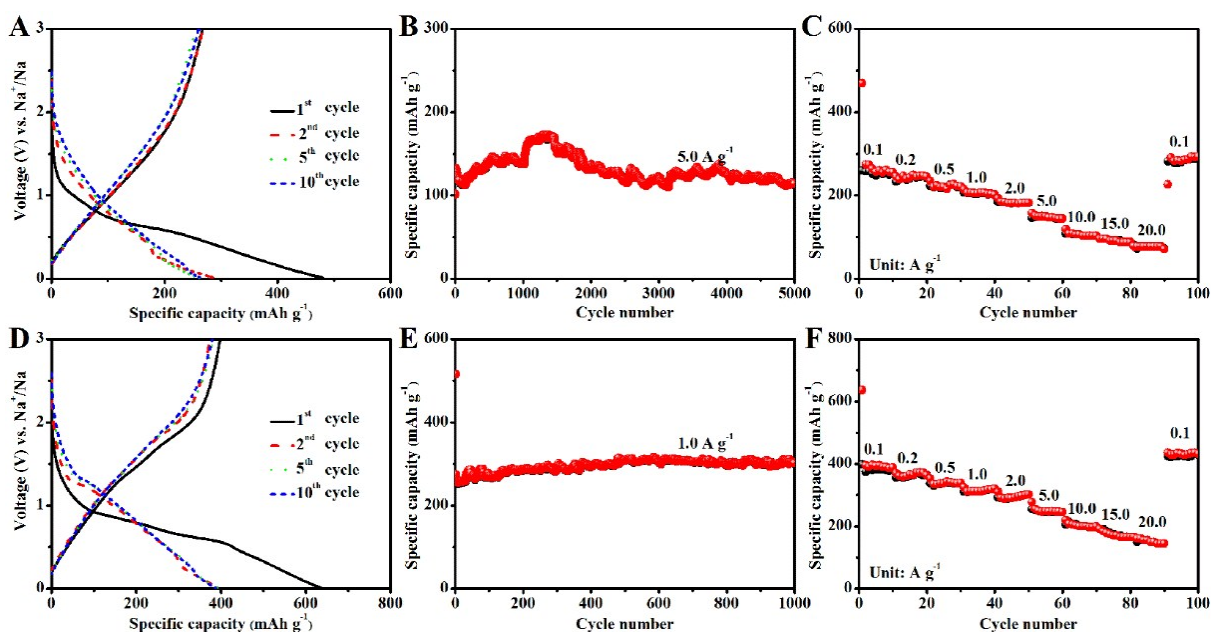


Figure S9. Nyquist plots of C@FeSe<sub>2</sub> electrode before and after cycling at 0.1 A g<sup>-1</sup>.



**Figure S10.** Sodium storage performance of the bowl-like C@Fe<sub>3</sub>O<sub>4</sub> and C@FeP hollow particles: (A) Discharge/charge profiles at the current density of 0.1 A g<sup>-1</sup>, (B) Cycling stability at the rate of 5.0 A g<sup>-1</sup>, (C) Rate capability under current densities ranging from 0.1 to 20 A g<sup>-1</sup> for bowl-like C@Fe<sub>3</sub>O<sub>4</sub> hollow particle anode; (D) Discharge/charge profiles at the current density of 0.1 A g<sup>-1</sup>, (E) Cycling stability at the rate of 1.0 A g<sup>-1</sup> (F) Rate capability under current densities ranging from 0.1 to 20 A g<sup>-1</sup> for bowl-like C@FeP hollow particle anode.

The sodium storage properties of the C@Fe<sub>3</sub>O<sub>4</sub> and C@FeP bowls as anode were also investigated. As shown in **Figure S10A**, the galvanostatic discharge/charge profiles at the rate of 0.1 A g<sup>-1</sup> demonstrate that the bowl-like C@Fe<sub>3</sub>O<sub>4</sub> hollow particle anode can deliver an initial capacity of 481 mA h g<sup>-1</sup> with a coulombic efficiency of 55.5%, while for the successive second, fifth and tenth cycles, the charge/discharge curves are almost coincident with each other, exhibiting the highly reversible sodium storage process. **Figure S10B** indicates the excellent cycling stability of bowl-like C@Fe<sub>3</sub>O<sub>4</sub> anode, where a high capacity retention can be achieved after 5000 cycles at the high rate of 5 A g<sup>-1</sup>. The rate performance (**Figure S10C**) indicates that the specific capacities are 275, 252, 227, 207, 185, 151, 96, 78 and 63 mA h g<sup>-1</sup>, respectively, when the current densities increasing from 0.1 to 20 A g<sup>-1</sup>. Moreover, when the current density returns to 0.1 A g<sup>-1</sup> from 20 A g<sup>-1</sup>, a higher capacity of 290 mA h g<sup>-1</sup> could be recovered. The electrochemical performance of bowl-like C@FeP hollow particle for sodium ion storage is given in **Figure S10D-F**. **Figure S10D** shows the galvanostatic discharge/charge profiles at 0.1 A g<sup>-1</sup>. The initial discharge and charge capacities are 637 and 397 mA h g<sup>-1</sup>, leading to an initial coulombic efficiency of 62.3%. The specific capacity is relatively stable at around 300 mA h g<sup>-1</sup> for 1000 cycles at the rate of 1A g<sup>-1</sup>. In addition, the bowl-like C@FeP anode could deliver an average capacity of 397, 373, 342, 319, 300, 256, 206 mA h g<sup>-1</sup>, 180 and 156 mA h g<sup>-1</sup>, respectively, corresponding to the current densities of 0.1, 0.2, 0.5, 1, 2, 5, 10, 15 and 20 A g<sup>-1</sup>.

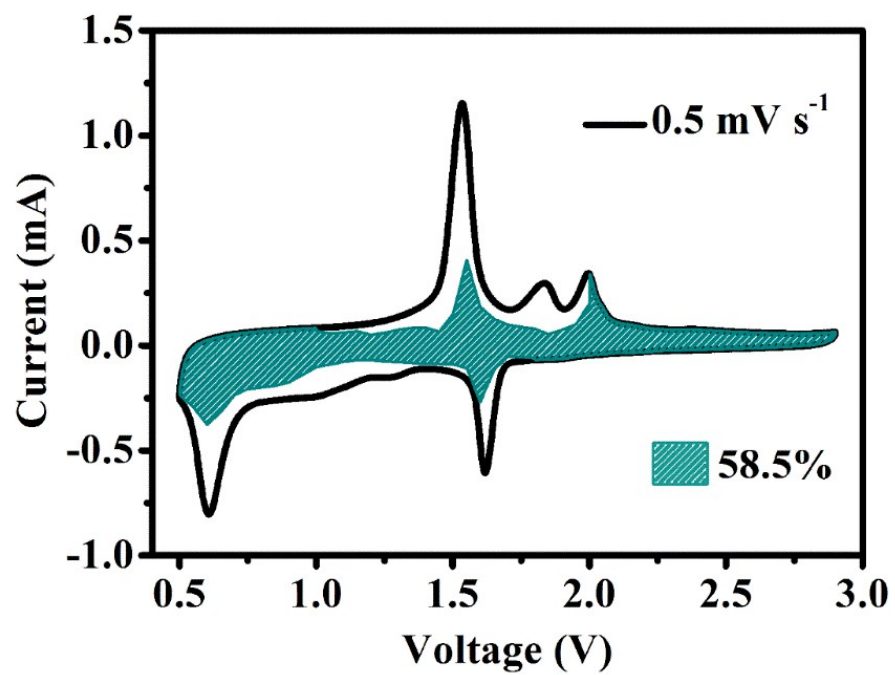
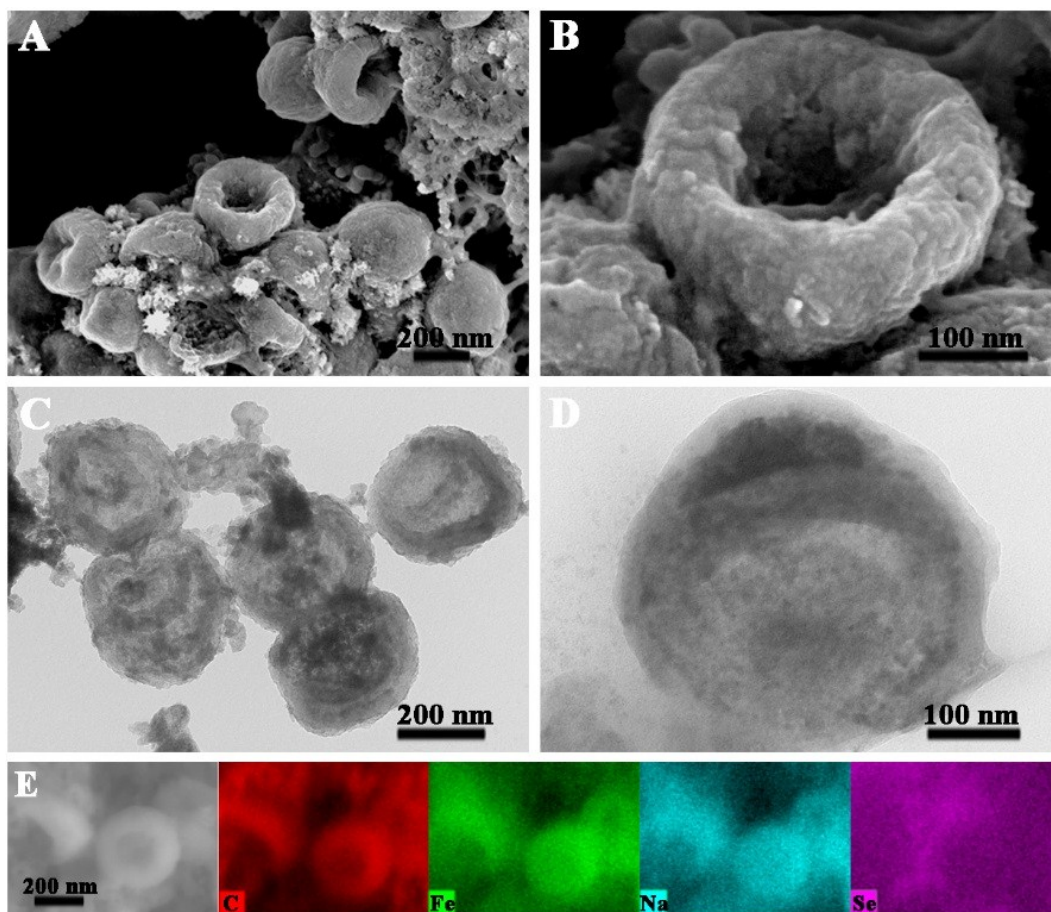
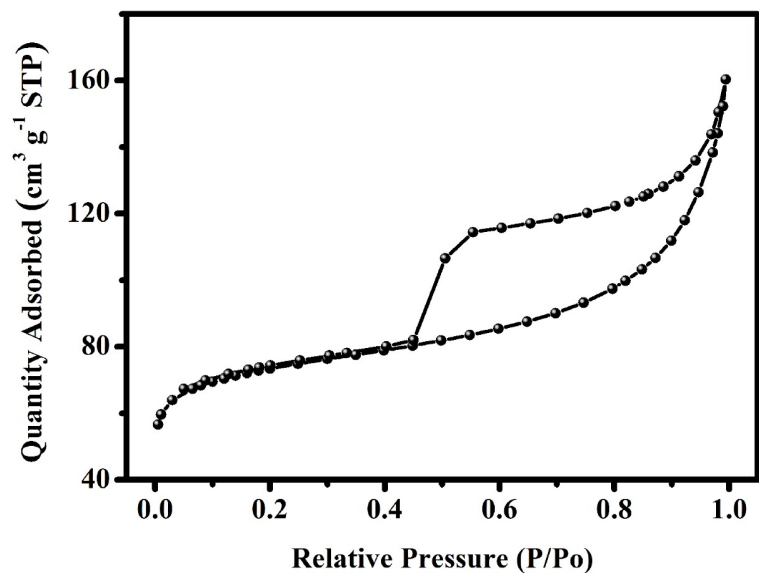


Figure S11. CV curve with the pseudocapacitive fraction shown by the shaded area at a scan rate of 0.5 mV s<sup>-1</sup>.



**Figure S12.** (a, b) SEM images, (c, d) TEM images and (e) corresponding elemental mapping results of C@FeSe<sub>2</sub> bowls after 120 cycles at the rate of 0.1 A g<sup>-1</sup>.



**Figure S13.** N<sub>2</sub> adsorption and desorption isotherms of C@FeSe<sub>2</sub> bowls. The BET surface area of C@FeSe<sub>2</sub> bowls is about 250.44 m<sup>2</sup> g<sup>-1</sup>.

1. H. Zhang, M. Yu, H. Song, O. Noonan, J. Zhang, Y. Yang, L. Zhou and C. Yu, *Chem. Mater.*, 2015, **27**, 6297-6304.